Journal of Physics: Conference Series **535** (2014) 012013 doi:10.1088/1742-6596/535/1/012013

Anisotropic flows and the shear viscosity of the QGP within a transport approach

S. Plumari[a,b], G.L. Guardo[a,b], A. Puglisi[b], F. Scardina[a,b] and V. Greco[a,b]

[a] *Department of Physics and Astronomy, University of Catania, Via S. Sofia 64, I-95125 Catania (Italy)*

[b] *Laboratorio Nazionale del Sud, INFN-LNS, Via S. Sofia 63, I-95125 Catania (Italy)*

E-mail: salvatore.plumari@hotmail.it

Abstract. We study the build up of elliptic flow v_2 and high order harmonics v_n within a transport approach at fixed shear viscosity to entropy density ratio η/s and with initial state fluctuations. In particular we study the effect of a temperature dependent η/s for two different beam energies: RHIC for Au+Au at $\sqrt{s} = 200\,GeV$ and LHC for $Pb+Pb$ at $\sqrt{s} = 2.76\,TeV$. We find that for the two different beam energies considered the suppression of the elliptic flow and of higher harmonics $v_3(p_T)$ and $v_4(p_T)$ due to the viscosity of the medium have different contributions coming from the cross over or QGP phase. Moreover, we discuss the correlation between the initial spatial anisotropies ϵ_n and flow coefficients v_n. We observe that the elliptic flow v_2 is strongly correlated with initial eccentricity ϵ_2. While higher harmonics v_3 and v_4 are weakly correlated to their asymmetry measure in coordinate space ϵ_3 and ϵ_4.

1. Introduction

The experimental results accumulated in these years in the ultra relativistic heavy ion collisions (uRHICs) first in the experiments conducted at RHIC and more recently at the LHC has shown that the elliptic flow $v_2 = \langle cos(2\,\varphi_p)\rangle = \langle (p_x^2 - p_y^2)/(p_x^2 + p_y^2)\rangle$, is the largest ever observed in these uRHICs [1, 2]. The elliptic flow is a measurement of the momentum anisotropy of the emitted particles and it is an observable that encodes information about the transport properties of the matter created in these collisions. In particular it is an observable sensitive to the shear viscosity to entropy density ratio η/s. Theoretical calculations within viscous hydrodynamics [3, 4] and in the recent years also calculation performed within transport approach [5, 6, 7] have shown that this large value of v_2 is consistent with a matter with a very low shear viscosity to entropy density ratio η/s close to the conjectured lower bound for a strongly interacting system, with $\eta/s = 1/4\pi$ [8]. Moreover, both calculations have shown that the v_2 depends sensitively on η/s. Furthermore, in the recent years the possibility to measure experimentally the event-by-event angular distribution of emitted particle has made possible the measurement of higher harmonics $v_n = \langle cos(n\,\varphi_p)\rangle$ for $n > 2$. The comparison between event-by-event viscous hydrodynamical calculations and the experimental results for v_n seems to confirm a finite but not too large value of $4\pi\eta/s \sim 1 - 3$ [9, 10]. However, small value of $\eta/s \sim 1/4\pi$ is not an evidence of the creation of a QGP phase. A phenomenological estimation of its temperature dependence could give information if the matter created in these collisions undergoes a phase transition [11, 12].

Information about a temperature dependence of η/s can be achieved studying the $v_2(p_T)$ and the high order harmonic $v_n(p_T)$ in wider range of energies. Similar studies have been performed using a transport approach but only for the elliptic flow [13].

There are several theoretical indications that η/s should have a particular behavior with the temperature[11, 12, 14, 15, 16, 17]. As an example in Fig.(1) it is shown a collection of theoretical results about the temperature dependence of η/s. Fig.(1) shows that in general η/s should have a typical behavior of phase transition with a minimum close to the critical temperature T_C [11, 12]. On one hand at low temperature estimations of η/s performed in

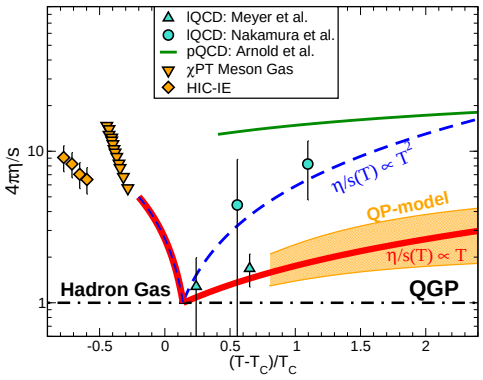

Figure 1. Different parametrizations for η/s as a function of the temperature. The orange area refers to the quasi-particle model predictions for η/s [18]. The different lines indicate different possible T dependencies while green line represents the result for the pQCD calculation [19]. Symbols are as in the legend. See the text for more details.

the chiral perturbation theory for a meson gas [14, 15], have shown that in general η/s is a decreasing function with the temperature, see down-triangles in Fig.(1). Similar results for η/s have been extrapolated from heavy-ion collisions at intermediate energies, see HIC-IE diamonds in Fig.(1). On the other hand at higher temperature $T > T_c$ lQCD calculation have shown but with large error bars that in general η/s becomes an increasing function with the temperature [16], see up-triangles and circles in Fig.(1). In general due to the large error bars in the lQCD results for η/s it is not possible to infer a clear temperature dependence in the QGP phase. The analysis at different energies of $v_2(p_T)$ and the extension to high order harmonics $v_n(p_T)$ can give further information about the T dependence of η/s. In this proceeding we will show some new results on $v_n(p_T)$ for the two different systems $Au + Au$ at $\sqrt{s} = 200\,GeV$ and $Pb + Pb$ at $\sqrt{s} = 2.76\,TeV$.

2. Kinetic approach at fixed shear viscosity to entropy density ratio

In this section we introduce a transport approach in which it is possible to fix the η/s ratio. This approach provides a tool to estimate the viscosity of the plasma valid in a wider range of η/s and p_T than hydrodynamical framework. We perform such simulations using a relativistic transport code developed in these years to perform studies of the dynamics of heavy-ion collisions at both RHIC and LHC energies [5, 7, 20, 21, 22]. The evolution of the phase-space distribution function $f(x, p, t)$ is given by solving the Relativistic Boltzmann Transport (RBT) equation:

$$p^\mu \, \partial_\mu f(x,p) = \int d\Gamma_2 d\Gamma_{1'} d\Gamma_{2'} (f_{1'} f_{2'} - f f_2) |\mathcal{M}|^2 \delta^4(p + p_2 - p_{1'} - p_{2'}) \; , \tag{1}$$

where $d\Gamma_k = d^3p_k/2E_k(2\pi)^3$ and $\mathcal{M}$ denotes the transition amplitude for the elastic processes which is directly linked to the differential cross section $|\mathcal{M}|^2 = 16\pi\, s\,(s - 4M^2) d\sigma/dt$ with s the Mandelstam invariant. Numerically we solve the RBT equation using the so called test particle method and the collision integral is solved by using Monte Carlo methods based on the stochastic interpretation of transition amplitude [23, 5, 21].

In order to study the dynamical evolution of the fireball with a certain $\eta/s(T)$ we determine locally in space and time the total cross section σ_{tot} needed to have the wanted local viscosity.

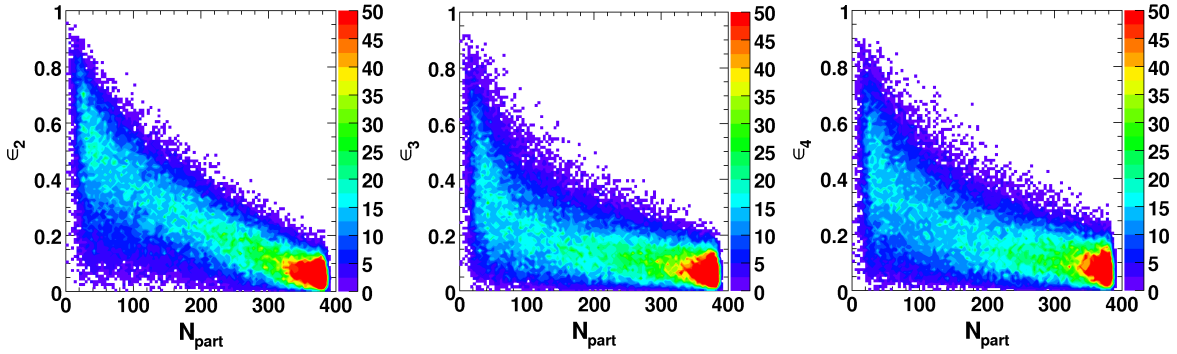

Figure 2. In the left, middle and right panel it is shown the coefficient ϵ_n as a function of the participant nucleons N_{part} respectively for $n = 2, 3$ and 4.

In the Chapmann-Enskog theory and for a pQCD inspired cross section, typically used in parton cascade approaches [24, 25, 5, 26, 27, 23, 6], with $d\sigma/dt \sim \alpha_s^2/(t - m_D^2)^2$, the η/s is given by the following expression:

$$\eta/s = \frac{1}{15}\langle p\rangle\,\tau_\eta = \frac{1}{15}\frac{\langle p\rangle}{g(a)\sigma_{tot}\rho}\,, \tag{2}$$

where $a = m_D/2T$, with m_D being the screening mass regulating the angular dependence of the cross section, while $g(a)$ is the proper function accounting for the pertinent relaxation time $\tau_\eta^{-1} = g(a)\sigma_{tot}\rho$ associated to the shear transport coefficient and it is given by:

$$g(a) = \frac{1}{50}\int dy y^6 \left[(y^2+\frac{1}{3})K_3(2y) - yK_2(2y)\right] h\left(\frac{a^2}{y^2}\right), \tag{3}$$

where K_n-s are the Bessel functions and the function h relate the transport cross section to the total cross section $\sigma_{tr}(s) = \sigma_{tot}\, h(m_D^2/s)$ with $h(\zeta) = 4\zeta(1+\zeta)[(2\zeta+1)ln(1+1/\zeta) - 2]$. Therefore the total cross section is evaluated locally by mean the Eq.(2).

3. Initial conditions

Our simulations start at the initial time $\tau_0 = 0.6 fm/c$. The initial conditions are longitudinal boost invariant. In the following discussion, we will consider two different types of initial conditions in coordinate space. One of them consist in a fixed distribution in transverse plane by using the standard Glauber model as used in previous works, see [5, 7, 20, 13]. The second one consist of an initial profile changing event by event that will be described below.

In order to generate an event by event initial profile we use the Monte-Carlo Glauber model to obtain the initial density distribution for each event. Woods-Saxon distribution is used to sample the nucleons randomly in the two colliding nucleus. In this way we generate a discrete distribution for these nucleons. We employ a geometrical method to determine if the two nucleons one for the nucleus A and the other one for the nucleus B are colliding: two nucleons collide each other if the relative distance in the transverse plane is $d_T \leq \sqrt{\sigma_{NN}/\pi}$ where σ_{NN} is the nucleon-nucleon cross section. The calculation of N_{coll} and N_{part} is given by counting the number of collisions and the number of participating nucleons for each event. In this way the position of the participating nucleons will fluctuate from event-to-event. The discrete distribution for the nucleons is converted to a smooth one by assuming for each nucleon a gaussian distribution centered in the nucleon position. Finally, the density in the transverse

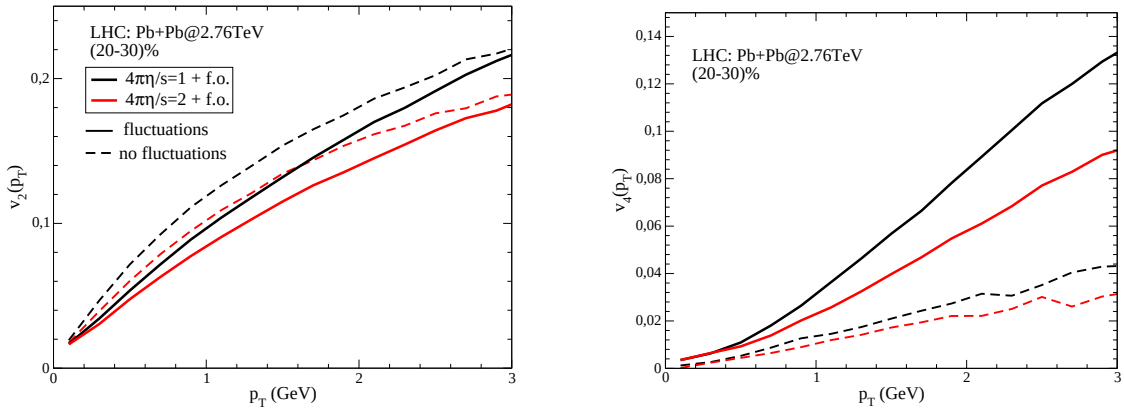

Figure 3. Left: differential elliptic flow $v_2(p_T)$ at midrapidity and for $(20-30\%)$ centrality. The black and red solid lines refer to the case with fluctuations and for $4\pi\eta/s = 1 + f.o.$ and $4\pi\eta/s = 2 + f.o.$ respectively. Term f.o. means the increase of η/s at lower temperature. The black and red dashed lines are for the case without fluctuations in the initial geometry. Right: differential $v_4(p_T)$ at midrapidity and for $(20-30\%)$ centrality with the same legend as in the left panel.

plane is given by the following sum

$$\rho_T(x,y) \propto \sum_{i=1}^{N_{part}} \exp\left[-\frac{(x-x_i)^2+(y-y_i)^2}{2\sigma_{xy}^2}\right] \tag{4}$$

where σ_{xy} is the Gaussian width and in the following calculations it has been fixed to $\sigma_{xy} = 0.5\,fm$. Given $\rho_T(x,y)$ we can calculate the initial anisotropy in coordinate space. The initial anisotropy is quantified in terms of the following coefficients ϵ_n:

$$\epsilon_n = \sqrt{< r_T^n \cos(n\phi) >^2 + < r_T^n \sin(n\phi) >^2} / < r_T^2 > \tag{5}$$

where $r_T = \sqrt{x^2+y^2}$ and $\phi = arctan(y/x)$ are the polar coordinate in the transverse plane. In the following discussion we will concentrate on the fireball produced in $Au+Au$ at $\sqrt{s_{NN}} = 200\,GeV$ and $Pb+Pb$ at $\sqrt{s_{NN}} = 2.76\,TeV$. For the nucleon-nucleon cross section we have used $\sigma_{NN} = 42\,mb$ and $70\,mb$ respectively. Fig.(2) shows the ϵ_2, ϵ_3 and ϵ_4 as a function of the number of participant N_{part}.

For the initialization in momentum space at RHIC (LHC) energies we have considered for partons with transverse momentum $p_T \leq p_0 = 2\,GeV$ $(3\,GeV)$ a thermalized spectrum in the transverse plane with a maximum initial temperature $T_0 = 340\,MeV$ $(510\,MeV)$. While for partons with $p_T > p_0$ we have assumed the spectrum of non-quenched minijets according to standard NLO-pQCD calculations with a power law shape. The transverse momentum of the particles is distributed uniformly in the azimuthal angle.

4. Effects of η/s on the $v_n(p_T)$

In this section we discuss the results for the final $v_n(p_T)$ corresponding to the different initial configurations. Differential flow coefficients $v_n(p_T)$ are very sensitive observables to the transport properties of the medium like the ratio η/s and they can give us more informations about the matter created in the heavy ion collisions. In the following discussion with $v_n(p_T)$ we mean the root mean square $\sqrt{< v_n^2 >}$ as it has been done in experimental data using the event plane

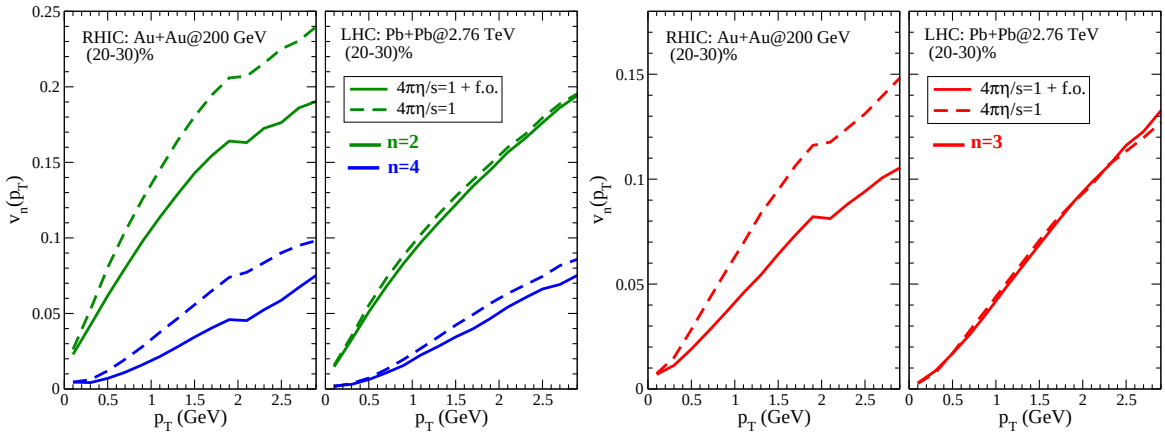

Figure 4. Left panel: differential $v_2(p_T)$ and $v_4(p_T)$ green and blue lines respectively at midrapidity and for $(20-30)\%$ collision centrality. The comparison is between the two systems: $Au+Au$ at $\sqrt{s}=200\,GeV$ and $Pb+Pb$ at $\sqrt{s}=2.76\,TeV$. The dashed lines refer to the case with a constant $\eta/s=(4\pi)^{-1}$ during all the evolution while the solid lines to the case with $\eta/s=(4\pi)^{-1}$ at higher temperature and with an increasing η/s ratio at lower temperature. Right panel: differential $v_3(p_T)$ red lines with the same legend as in the left panel.

method. In the left panel of Fig.(3) we compare the differential $v_2(p_T)$ obtained with an initial state fluctuations (solid lines) as discussed in the previous section with the one obtained for an event by event averaged initial profile (dashed lines). These results are for the system $Pb+Pb$ at $\sqrt{s}=2.76\,TeV$ and for $(20-30\%)$ centrality. For this collision centrality we have simulated $N_{event}=500$ events. We have checked the convergence of our results for the v_2, v_3 and v_4 with lattice spacing of the calculation grid and with the number of test particles. As shown in the left panel of Fig.(3) the fluctuations in the initial geometry reduce the elliptic flow of about 10%. In general the introduction of the fluctuations in the initial geometry play the role to generate the higher order harmonics in particular the odd harmonics which were absent in the averaged initial configuration by symmetry. Different behavior were observed for the 4-th harmonic as shown in right panel of Fig.(3)where in this case we have that the role of the fluctuation is to increase the $v_4(p_T)$ by a factor 2. This is due to the fact that ϵ_4 is almost completely generated by the fluctuations. Moreover, comparing the black and red solid lines with the dashed ones we observe that now the v_4 becomes more sensitive to the value of the viscosity.

In order to study the role of the η/s ratio on the build up of the elliptic flow $v_2(p_T)$ and on the high order harmonics $v_n(p_T)$ we have performed two different calculations: one with a constant $4\pi\eta/s=1$ during all the evolution of the system and the other one with $4\pi\eta/s=1$ at higher temperature in the QGP phase and an increasing η/s in the cross over region towards the estimated value for hadronic matter $4\pi\eta/s\approx 6$ as depicted in Fig.(1). Such an increase of η/s at lower temperature allows for a smooth realistic realization of the kinetic freeze-out. This last kind of calculation is labeled by f.o.. This is because at lower temperature, according to the formula Eq.(2), to account for the increase of η/s towards the estimated value for the hadronic matter, the total cross section decrease.

In the left panel of Fig.(4) it is shown the elliptic flow $v_2(p_T)$ and the $v_4(p_T)$ (green and blue lines) at mid rapidity for $(20-30)\%$ centrality for both RHIC $Au+Au$ at $\sqrt{s}=200\,GeV$ (left panel) and LHC $Pb+Pb$ at $\sqrt{s}=2.76\,TeV$ (right panel). In general in agreement with what has been obtained in hydrodynamical calculations, the increase of the viscosity of the medium has the effect to reduce the v_2 and v_4. As we can see at RHIC energies comparing the blue dashed

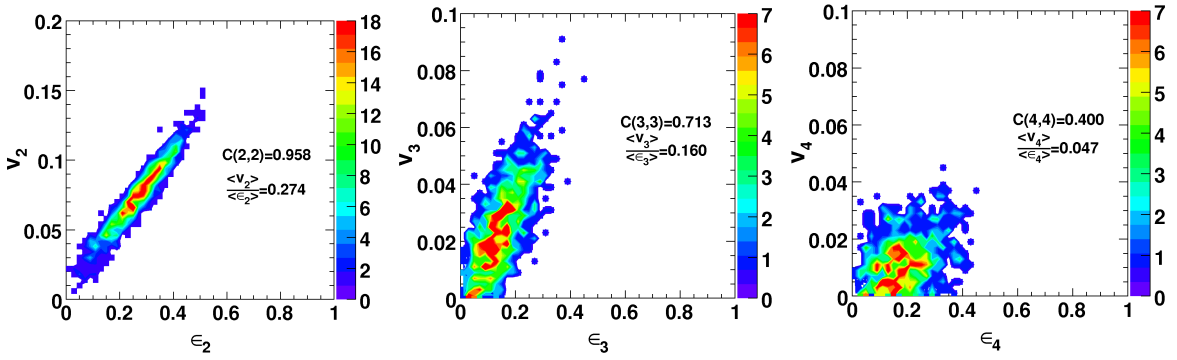

Figure 5. In the left, middle and right panel it is shown v_n and ϵ_n at mid rapidity and for $(20-30)\,\%$ respectively for $n = 2, 3$ and 4. In these calculations we have fixed $\eta/s = 1/(4\pi)$ during all the evolution of the system.

lines with the solid ones, in the left panel of Fig.(4), the $v_2(p_T)$ is sensitive to the increase of the η/s at lower temperature close to the cross over region. In particular the effect is a reduction of the elliptic flow of about 17%. A similar trend were observed for the 4-th harmonic $v_4(p_T)$ where we have a reduction due to the increase of η/s at lower temperature but the effect in this case is larger then the previous one of about 30%. The different sensitivity to the η/s can be attributed to their different formation time, $t_{v_4} > t_{v_2}$ [26]. On the other hand at LHC energies, left panel of Fig.(4), the scenario is different, the elliptic flow is almost unaffected by the increase of η/s ratio at low temperature (in the hadronic phase) as we can see comparing the green dashed line with the solid one. Instead we observe that the increase of η/s at lower temperature has a more sensitive effect on the $v_4(p_T)$ with a reduction of about 10%, see blue solid and dashed lines. Again this different sensitivity to the η/s in the cross over region between v_2 and v_4 at LHC are consistent with the results obtained at RHIC energies and related to the different formation time of the harmonics. The greater sensitivity at RHIC energies of both v_2 and v_4 to the η/s at low temperature is related to the different life time of the fireball. In fact the life time of the fireball at LHC is greater than that at RHIC, 8-10 fm/c at LHC against 4-5 fm/c at RHIC [28]. In general this means that at RHIC energies the v_n have not enough time to fully develop in the QGP phase. While at LHC energies we have that the v_n develops almost completely in the QGP phase and therefore it is less sensitive to the dynamics at lower T. In the right panel of Fig.(4) it is shown the triangular flow $v_3(p_T)$ (red lines) at mid rapidity for $(20-30)\%$ centrality and for both RHIC $Au+Au$ at $\sqrt{s} = 200\,GeV$ (left panel) and LHC $Pb+Pb$ at $\sqrt{s} = 2.76\,TeV$ (right panel). In agreement with what has been obtained for the even harmonics v_2 and v_4, we observe at RHIC energies a reduction of $v_3(p_T)$ due to the increase of the η/s at low temperature with a reduction of about 25%, while at LHC it is almost insensitive to the change of η/s in the cross over region.

5. Correlations between v_n and ϵ_n

In the recent years, the correlation between integrated v_2 and high order harmonics v_3, v_4 with the initial asymmetry in coordinate space ϵ_2, ϵ_3 and ϵ_4 has been studied in the event-by-event viscous hydrodynamics framework [29, 30, 31]. In general it has been shown that the elliptic flow is strongly correlated with initial eccentricity while a weaker correlation has been found for higher harmonics v_3, v_4 with ϵ_3 and ϵ_4. In this section we study these correlations within a transport approach with initial state fluctuation and for fixed η/s. In particular the results shown in this section are for an $\eta/s = 1/(4\pi)$ during all the evolution of the fireball.

In the left hand side of Fig.(5), we have shown the final integrated elliptic flow $< v_2 >$ as

a function of the corresponding initial eccentricity $< \epsilon_2 >$ for each event. We observe that for $20-30\%$ of centrality the elliptic flow results are strongly correlated with the initial eccentricity. This is consistent with a correlation coefficient close to 1. The correlation coefficient is given by:

$$C(y,x) = \frac{\sum_i (x_i - \langle x \rangle)(y_i - \langle y \rangle)}{\sqrt{\sum_i (x_i - \langle x \rangle)^2 \sum_i (y_i - \langle y \rangle)^2}} \tag{6}$$

For the plot in the left panel of Fig.(5)we get $C(2,2) \approx 0.96$. In the middle and right panel of Fig.(5), we have shown the results obtained for the higher harmonics $< v_3 >$ and $< v_4 >$ respectively and for $20-30\,\%$ centrality. We observe that the correlation between triangular flow $< v_3 >$ and its initial $< \epsilon_3 >$ is weaker then that between $< v_2 >$ and $< \epsilon_2 >$ with a correlation coefficient $C(3,3) \approx 0.71$. Furthermore for the fourth harmonic flow $< v_4 >$ we observe an uncorrelation with its initial $< \epsilon_4 >$ as shown by a correlation coefficient close to zero. One explanation for this no linear correlation between $< v_4 >$ and $< \epsilon_4 >$ is that the for final $< v_4 >$ there is also a correlation with the initial $< \epsilon_2 >$. In [31] has been shown it possible to have a good linear correlation between $< v_4 >$ and a linear combination of the initial $< \epsilon_2 >$ and $< \epsilon_4 >$.

6. Conclusions

We have investigated within an event-by-event transport approach at fixed η/s, the build up of $v_2(p_t)$ and higher harmonics $v_3(p_T)$ and $v_4(p_T)$ for two different beam energies: RHIC for $Au + Au$ at $\sqrt{s} = 200\,GeV$ and LHC for $Pb + Pb$ at $\sqrt{s} = 2.76\,TeV$. We have found that at RHIC the $v_n(p_T)$ are more sensitive to the value of η/s at low temperature and in particular this sensitivity increase with the order of the harmonics. At LHC we get a different effect, the $v_n(p_T)$ are not so sensitive to the increase of η/s at low temperature. Finally, we have studied also the relation between v_n and ϵ_n for $n = 2, 3$ and 4 in ultra relativistic heavy-ion collisions within an event-by-event relativistic transport approach. We have shown that the second and third harmonic flows are correlated to their initial eccentricities, a result similar to that has been obtained in the recent years in viscous hydrodynamics.

7. Acknowledgments

V.Greco, F. Scardina and G.L. Guardo acknowledge the support of the ERC-StG Grant under the QGPDyn project.

References

[1] Adams J *et al.* (STAR Collaboration) 2005 *Nucl.Phys.* **A 757** 102–183 (*Preprint* `nucl-ex/0501009`)
[2] Aamodt K *et al.* (ALICE Collaboration) 2010 *Phys.Rev.Lett.* **105** 252302 (*Preprint* `1011.3914`)
[3] Romatschke P and Romatschke U 2007 *Phys.Rev.Lett.* **99** 172301 (*Preprint* `0706.1522`)
[4] Song H and Heinz U W 2008 *Phys.Rev.* **C 78** 024902 (*Preprint* `0805.1756`)
[5] Ferini G, Colonna M, Di Toro M and Greco V 2009 *Phys.Lett.* **B 670** 325–329 (*Preprint* `0805.4814`)
[6] Xu Z and Greiner C 2009 *Phys.Rev.* **C 79** 014904 (*Preprint* `0811.2940`)
[7] Plumari S and Greco V 2012 *AIP Conf.Proc.* **1422** 56–61 (*Preprint* `1110.2383`)
[8] Kovtun P, Son D and Starinets A 2005 *Phys.Rev.Lett.* **94** 111601 (*Preprint* `hep-th/0405231`)
[9] Schenke B, Jeon S and Gale C 2012 *Phys.Rev.* **C 85** 024901 (*Preprint* `1109.6289`)
[10] Gale C, Jeon S, Schenke B, Tribedy P and Venugopalan R 2013 *Phys.Rev.Lett.* **110** 012302 (*Preprint* `1209.6330`)
[11] Csernai L P, Kapusta J and McLerran L D 2006 *Phys.Rev.Lett.* **97** 152303 (*Preprint* `nucl-th/0604032`)
[12] Lacey R A, Ajitanand N, Alexander J, Chung P, Holzmann W *et al.* 2007 *Phys.Rev.Lett.* **98** 092301 (*Preprint* `nucl-ex/0609025`)
[13] Plumari S, Greco V and Csernai L 2013 (*Preprint* `1304.6566`)
[14] Prakash M, Prakash M, Venugopalan R and Welke G 1993 *Phys.Rept.* **227** 321–366
[15] Chen J W, Li Y H, Liu Y F and Nakano E 2007 *Phys.Rev.* **D 76** 114011 (*Preprint* `hep-ph/0703230`)
[16] Meyer H B 2007 *Phys.Rev.* **D 76** 101701 (*Preprint* `0704.1801`)

[17] Das S K and Alam J e 2011 *Phys.Rev.* **D 83** 114011 (*Preprint* 1011.4181)
[18] Plumari S, Alberico W M, Greco V and Ratti C 2011 *Phys.Rev.* **D 84** 094004 (*Preprint* 1103.5611)
[19] Arnold P B, Moore G D and Yaffe L G 2003 *JHEP* **0305** 051 (*Preprint* hep-ph/0302165)
[20] Plumari S, Puglisi A, Colonna M, Scardina F and Greco V 2013 *J.Phys.Conf.Ser.* **420** 012029 (*Preprint* 1209.0601)
[21] Plumari S, Puglisi A, Scardina F and Greco V 2012 *Phys.Rev.* **C 86** 054902 (*Preprint* 1208.0481)
[22] Ruggieri M, Scardina F, Plumari S and Greco V 2013 *Phys.Lett.* **B 727** 177–181 (*Preprint* 1303.3178)
[23] Xu Z and Greiner C 2005 *Phys.Rev.* **C 71** 064901 (*Preprint* hep-ph/0406278)
[24] Zhang B, Gyulassy M and Ko C M 1999 *Phys.Lett.* **B 455** 45–48 (*Preprint* nucl-th/9902016)
[25] Molnar D and Gyulassy M 2002 *Nucl.Phys.* **A 697** 495–520 (*Preprint* nucl-th/0104073)
[26] Greco V, Colonna M, Di Toro M and Ferini G 2008 *Prog.Part.Nucl.Phys.* (*Preprint* 0811.3170)
[27] Plumari S, Baran V, Di Toro M, Ferini G and Greco V 2010 *Phys.Lett.* **B 689** 18–22 (*Preprint* 1001.2736)
[28] Aamodt K *et al.* (ALICE Collaboration) 2011 *Phys.Lett.* **B 696** 328–337 (*Preprint* 1012.4035)
[29] Niemi H, Denicol G, Holopainen H and Huovinen P 2013 *Phys.Rev.* **C 87** 054901 (*Preprint* 1212.1008)
[30] Chaudhuri A, Haque M R, Roy V and Mohanty B 2013 *Phys.Rev.* **C 87** 034907 (*Preprint* 1211.2040)
[31] Gardim F G, Grassi F, Luzum M and Ollitrault J Y 2012 *Phys.Rev.* **C 85** 024908 (*Preprint* 1111.6538)